Proceedings of the
Annual Stability Conference
Structural Stability Research Council
Charlotte, North Carolina, April 11-14, 2023

Refined Design Expression for the In-Plane Girder Stiffness of Torsional Beam Bracing Systems

David J. Fish[1], Sunghyun Park[2], Todd A. Helwig[3], Michael D. Engelhardt[4]

Abstract

Local and global stability are a major concern during erection and construction of steel bridge systems. Global stability is usually controlled by conventional lateral-torsional buckling (LTB), which is enhanced by reducing the unbraced length of the girders by cross-frames spaced along the length of bridge. Cross-frames fit into the category of torsional bracing since the braces restrain twist of the girder cross-sections. Effective bracing must satisfy both stiffness and strength requirements. The stiffness of cross-frames is a function of several components: including the stiffness of the brace, cross-sectional distortion, and the in-plane stiffness of the girders. While the current bracing provisions in the AISC Specification do not include the in-plane girder stiffness, this stiffness component can dominate the behavior of narrow girder units and may lead to inadequate bracing if not considered. Recently approved provisions in the AASHTO Specification make use of a relatively simple expression developed in the 1990's for evaluating the girder in-plane stiffness, however, the accuracy of the expression for many bridge systems is not clear. This paper summarizes an on-going study focused on improved bracing design guidance considering the in-plane stiffness of the girders. The work focuses on the warping rigidity of multi-girder systems and extends findings from previous investigations that have targeted the system-buckling mode of narrow girder systems. The paper focuses on eigenvalue buckling solutions to demonstrate the stiffness behavior of torsional bracing.

1. Introduction

I-shaped girders are often utilized in steel bridge systems, as they can offer structural efficiency and economy in many applications. However, the high strength-to-weight ratio of steel can lead to relatively slender elements and systems, requiring careful consideration of stability during erection and other construction phases. During these phases, the non-composite steel section alone supports the entire load. The critical limit state under these construction conditions is usually lateral-torsional buckling (LTB), which is a limit state that involves lateral movement of the compression flange and twist of the section.

[1] Graduate Research Assistant (University of Texas at Austin) and Design Engineer, Texas Department of Transportation, <david.fish@txdot.gov>
[2] Post-Doctoral Researcher, University of Texas at Austin, <pssing0926@gmail.com>
[3] Jewel McAlister Smith Professorship, University of Texas at Austin, <thelwig@mail.utexas.edu>
[4] Adnan Abou-Ayyash Centennial Professorship, University of Texas at Austin, <mde@mail.utexas.edu>

The LTB behavior of a girder can be improved by reducing its unbraced length. Effective beam bracing can be achieved by either restraining lateral displacement of the critical compression flange (lateral bracing), or by controlling twist of the section (torsional bracing). After a composite deck has been poured and cured, the deck generally provides both lateral and torsional restraint to the girders. As a result, conventional LTB is not typically a concern in the finished structure. In I-girder bridge systems, torsional braces (such as cross-frames or diaphragms) typically serve as the stability braces during construction to enhance the LTB resistance of the girders.

Effective bracing must satisfy both stiffness and strength requirements (Winter, 1960). The stiffness of torsional bracing systems is a function of the stiffness of the brace, cross-sectional distortion, as well as the in-plane stiffness of the girders.

An in-plane girder stiffness expression was developed in the early 1990's (Helwig, Yura and Frank, 1993) and was derived for a twin-girder system with a single intermediate torsional brace at mid-span. Recent experience utilizing this expression suggested that there are some cases in which the in-plane girder stiffness is over-predicted by this expression when compared to FEA solutions. Because in-plane girder stiffness can be the limiting factor in girder system stability analyses, it was deemed necessary to investigate the in-plane girder stiffness component to better understand its impact on the bridge behavior.

The objective of this research is to develop a refined expression that more accurately accounts for the in-plane girder stiffness component of the total system stiffness of torsional braces in a steel bridge system. The investigation is focused on the impact that the number of both intermediate cross-frames and girders have on the in-plane girder stiffness of a given girder system. The study has been divided into two phases with the first phase focused on deriving a suitable in-plane stiffness expression based upon the system/global buckling mode of the girders. More recently, the second phase of the study has focused on verifying the accuracy and potential modifications of the phase 1 expression for predicting the torsional brace stiffness within a girder system.

2. Background

While the lateral-torsional buckling (LTB) resistance can be improved by adjusting girder proportions, the most efficient means of increasing buckling resistance is generally by reducing the unbraced length of the member. For individual girders, the unbraced length is the distance between bracing locations, which is often highly variable during the erection process. Effective bracing can be achieved by controlling lateral movement of the compression flange (lateral bracing) or by controlling twist of the section (torsional bracing). The focus of this investigation is on torsional bracing, which is the most common bracing utilized in steel bridge applications. The bracing of steel bridge systems is most often provided by cross-frames or plate diaphragms that frame between adjacent girders. Although historically, the unbraced length was taken as the spacing between cross-frames and diaphragms, Yura et. al (2008) identified situations where girder systems can buckle in a half-sine curve along the entire span. The buckling mode is not significantly impacted by the spacing between cross-frames and is commonly referred to as System or Global Buckling. The following two sub-sections distinguish between conventional LTB and the System modes of buckling.

2.1 Conventional Lateral-Torsional Buckling

Conventional LTB is a failure mode that generally consists of a lateral translation of the section accompanied by a twist of the entire section. Although there are isolated cases, such as unbraced cantilevers when the tension flange may have the largest lateral deformation, the compression flange generally experiences the largest magnitude of lateral displacement. With suitable bracing, lateral torsional buckling generally occurs between bracing locations, i.e., over the unbraced length. Timoshenko (Timoshenko and Gere, 1961) derived the following exact elastic buckling solution for a simply supported, doubly symmetric section, accounting for both St. Venant and warping torsional stiffness, for the case of uniform moment loading:

$$M_{cr} = \frac{\pi}{L_b}\sqrt{EI_y GJ + \frac{\pi^2 E^2 C_w I_y}{L_b^2}} \tag{1}$$

where E is the modulus of elasticity, I_y is the weak-axis moment of inertia, L_b is the unbraced length, G is the shear modulus of elasticity, J is the torsional constant, and C_w is the torsional warping constant as estimated by Eq. 2:

$$C_w = \frac{I_y h_o^2}{4} \tag{2}$$

where h_o is the distance between flange centroids.

Considering the two terms under the radical in Eq. 1, the first is related to the St. Venant torsional stiffness and is related to the uniform torsional resistance of the section. The second term is related to warping stiffness as well as to the non-uniform torsional stiffness. In the original derivation of Eq. 1, Timoshenko stated that both twist and lateral deformation were restrained at the brace points and that warping was unrestrained at the ends of the unbraced length; however, only the boundary condition of zero twist was enforced in the derivation. Therefore, solely preventing twist of the cross-section results in effective bracing against LTB. Bracing can also be achieved by stopping lateral deformation of the compression flange (lateral bracing), which also essentially stops twist of the section since the lateral deformation of the compression element generally leads to twist of the section.

2.2 System (Global) Buckling

The system, or global, form of LTB has been the focus of several research studies since the early 2000's. The studies stemmed from the collapse of one bridge and near collapse of other bridges during the construction. System LTB occurs when the girder system is interlinked by braces, such as cross-frames, and the overall system buckles as a unit. This mode often becomes more critical than conventional LTB (buckling between brace points) in narrow girder systems with larger L_g/W ratios; where L_g is the span length and W is the girder system width. Yura et al. (2008) developed an expression for the elastic global buckling resistance of a doubly symmetric twin I-girder system, which is shown in Eq. 3:

$$M_g = \frac{2\pi}{L_g}\sqrt{EI_yGJ + \frac{\pi^2 E^2 I_y}{4L_g^2}\left(I_y h_o^2 + I_x s^2\right)} \tag{3}$$

where I_x is the strong-axis moment of inertia, s is the girder spacing and all other variables are as previously defined. All section properties in Eq. 3 (I_x, I_y, J, h_o) are those for a single girder.

This expression is similar in form to Eq. 1 and incorporates many of the same basic assumptions. However, an additional assumption, critical to the development of this expression, is that the torsional braces have enough in-plane stiffness to maintain the same twist angle for both girders (as shown in Fig. 1):

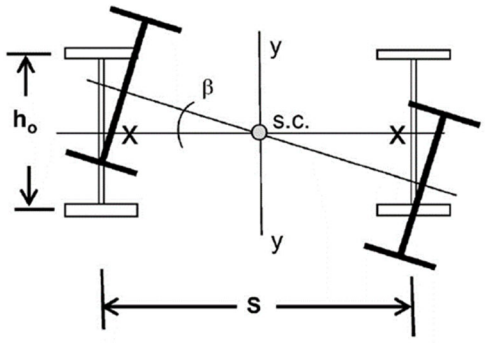

Figure 1: Rigid Body Rotation with Cross-Frame Omitted (Adapted from Yura et al., 2008)

In girders with typical proportions, the St. Venant term in Eq. 3 does not significantly impact the behavior. Neglecting this term, Yura et al. (2008) produced the simplified expression shown in Eq. 4, which gives the simplified buckling moment capacity for a single girder in a twin-girder system:

$$M_{gs} = \frac{\pi^2 sE}{2L_g^2}\sqrt{I_y I_x} \tag{4}$$

Accounting for moment gradient, singly symmetric girder sections, and multiple girders within the system, Yura et al. (2008) modified Eq. 4 in to produce the expression shown in Eq. 5:

$$M_{gls} = C_b \frac{\pi^2 (n_g - 1) sE}{n_g L_g^2}\sqrt{I_{eff} I_x} \tag{5}$$

where C_b is the moment gradient factor, n_g is the number of girders in the system, I_{eff} is the effective weak-axis moment of inertia (Yura, 2001) and all other variables are as previously defined.

Yura et al. (2008) applied similar modifications, as shown in Eq. 5, to Eq. 3. However, these adjustments only account for the in-plane flexural stiffness of the two exterior girders. Though this is a conservative approach, it provides an avenue for further refinement.

2.3 General Bracing Requirements

The concept that effective stability braces must have both adequate stiffness and strength was first demonstrated by Winter (1960). Winter developed a model that demonstrated a simple means of determining the ideal stiffness requirements for lateral bracing systems. The ideal stiffness is the minimum stiffness required that allows a member to reach a load level corresponding to buckling between the brace points. Winter's model also demonstrated the impact of imperfections on the buckling behavior, and that a stiffness larger than the ideal stiffness was necessary to control member deformations and brace forces. As a result, most bracing provisions currently recommend using twice the ideal stiffness. Considering Winter's model for lateral bracing of columns, providing twice the ideal stiffness results in the deformation of the column at the brace location to be equal in magnitude to that of the initial imperfection, Δ_o (i.e., $\Delta_{total} = 2\Delta_o$). Limiting the magnitude of the initial imperfection is important because the forces within the brace are directly related to its magnitude (Yura, 2001). Although Winter's work focused on lateral bracing systems, the dual criteria of stiffness and strength are valid for all stability bracing systems, including torsional beam bracing.

The initial imperfection assumed in the development of the current AISC design provision expressions is based on allowable fabrication and construction tolerances for girder out-of-straightness, as established by the AISC Code of Standard Practice (2022). The effect of initial imperfection on torsional bracing was studied by Wang and Helwig (2005). They demonstrated that, in bridge girders, the critical imperfection (i.e., the imperfection that maximizes force demands on the braces) usually involves a lateral sweep of the compression flange, with the tension flange remaining straight (un-displaced laterally). This effectively produces an initial twist of the cross-section. Using a sweep tolerance as $L/1000$ – with a brace at midspan, the sweep would be $2L_b/1000 = L_b/500$. Therefore, for the critical imperfection (Helwig and Wang, 2003), the magnitude of the initial twist imperfection is:

$$\theta_o = \frac{L_b}{500 h_o} \tag{6}$$

where L_b is the spacing between torsional braces.

2.4 Torsional Bracing Requirements

The torsional beam bracing provisions in AISC (2016) provide stiffness and strength requirements that are a function of the design moment, M_u. The design moment that the brace should be designed for in a bridge will be the moment in the girder that the brace must provide stability to. As noted earlier, the critical stage for LTB stability is generally during casting of the concrete deck. Therefore, M_u will be the maximum factored construction moment during casting of the slab. The stiffness provisions in AISC (2016) are given by the following expression:

$$\beta_{T,req} = \frac{2.4 L_g M_u^2}{\Phi C_{bb}^2 n_{cf} E I_{eff}} \tag{7}$$

where Φ is the stability bracing resistance factor, C_{bb} is the moment gradient factor within the critical unbraced beam or girder, and n_{cf} is the number of intermediate cross-frames.

The provided brace stiffness ($\beta_{T,act}$) must be equal to or greater than the required system stiffness of Eq. 7, as shown in Eq. 8:

$$\beta_{T,act} \geq \beta_{T,req} \tag{8}$$

As noted earlier, the system stiffness is a function of several bracing components including the stiffness of the brace (β_b), cross sectional distortion (β_{sec}), and the in-plane girder stiffness (β_g). Like many bracing systems, torsional bracing follows the fundamental equation for springs in series, such that the actual torsional system stiffness is given by the following expression:

$$\frac{1}{\beta_{T,act}} = \frac{1}{\beta_b} + \frac{1}{\beta_{sec}} + \frac{1}{\beta_g} \tag{9}$$

There are a number of sources that discuss the brace stiffness and the effects of cross-sectional distortion (AISC 2016, Yura 2001). The focus of the research in this paper is on the in-plane girder stiffness component, which is discussed in more detail in the next section.

2.4 In-Plane Girder Stiffness

When multiple girders are connected by bracing, such that they act as a unit, the in-plane (i.e., major axis) flexural stiffness of the individual girders contribute to the determination of overall stiffness of the torsional bracing system. The stiffness contribution of the girders was first investigated for twin-girder systems by Helwig, Yura, and Frank (1993). As shown in Fig. 2 when the girders are subjected to a twist, the internal moment that is subsequently developed in the cross-frame is equilibrated by vertical shear forces acting at the ends of the brace. The vertical forces on the adjacent girders cause one girder to deflect upwards and the other to deflect downwards leading to a rigid body rotation. These deformations reduce the effectiveness of the brace. With a wider system, this displacement is reduced, as demonstrated by the four-girder system shown in the figure.

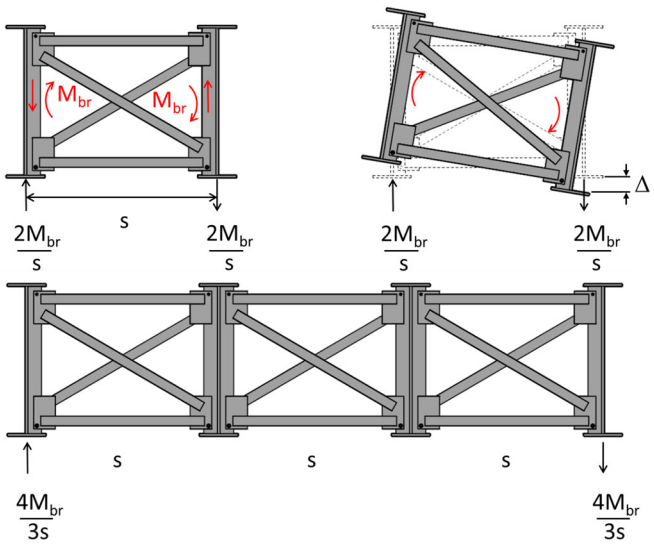

Figure 2: In-Plane Girder Stiffness (Fish, 2021)

This behavior was initially quantified by Helwig, Yura and Frank (1993) for a two-girder system and was expanded to multiple-girder systems by Yura (2001) as shown in Eq. 10:

$$\beta_{g,current} = \frac{24(n_g - 1)^2 s^2 E I_x}{n_g L^3} \tag{10}$$

The in-plane girder stiffness contribution is generally the most significant in narrow systems, such as two or three-girder bridges, and is tied to the system buckling mode, which was discussed in Section 2.2 (Yura et al., 2008; Han and Helwig, 2016). Considering Eq. 9, if β_g is less than $\beta_{T,req}$, full bracing cannot be achieved, regardless of the stiffness of the brace that is utilized. This situation is closely tied to the system buckling mode. From a buckling perspective, if the in-plane stiffness of the girder is insufficient, the system mode will generally control over buckling between the brace points. Because the system mode of buckling is closely tied to the in-plane stiffness requirements, a system mode approach is a logical methodology for deriving a more accurate expression. The following section outlines a potential expression for consideration.

3. Derivation of a Refined In-Plane Girder Stiffness Expression

The derivation of the expression for the in-plane girder stiffness is outlined in Fish (2021). The expression was developed considering the input of multiple girders interconnected by cross-frames or plate diaphragms. The derivation made use of the buckling solution for continuously torsionally-braced girders developed by Taylor and Ojalvo (1966), given in the following expression:

$$M_{cr} = \sqrt{M_o^2 + \bar{\beta}_T E I_y} \tag{11}$$

where M_o is the buckling capacity of an unbraced girder which is equal to the M_{cr} of Eq. (1), $\bar{\beta}_T$ is the continuous torsional brace stiffness (units of moment/rad/unit length), and the other variables are as previously defined.

A refined system buckling expression was developed that accounted for all of the girders' in-plane stiffness contributions. This expression was set equal to the Taylor and Ojalvo expression (Eq. 11) providing an explicit solution for the in-plane girder stiffness.

3.1 Derivation of a Refined System Buckling Capacity Expression

The differential equations used in the development of Timoshenko's buckling expression (Eq. 1) are equally applicable for multiple girder systems if the same basic assumptions are met (Yura et al., 2008). In order to satisfy these assumptions for multi-girder systems, a few modifications of Eq. 1 are necessary. The effect of multiple girders was accounted for by evaluating the lateral bending, torsional, and warping rigidities of the system. Three assumptions, associated with the bracing (cross-frames in this case), must also be considered:

1. The cross-frames are stiff enough in their own plane that they maintain the same angle of twist for adjacent girders (Fig. 1).

2. The cross-frame members are assumed to act as truss members (pin-connected) thereby precluding Vierendeel truss action.

3. There are enough cross-frames along the length of the girder that the rigid body rotation described by Fig. 1 can be assumed along the entire length (no system distortion).

There were a few adjustments made to the aforementioned rigidity components. The lateral bending system rigidity is simply a summation of the lateral-bending rigidities of the individual girders and is, therefore, the rigidity of a single girder multiplied by the number of girders in the system ($n_g EI_y$). The same is true for both the uniform torsional system rigidity ($n_g GJ$) and the lateral-warping system rigidity ($n_g EC_w$).

The adjustment to, what is being called, the vertical warping system rigidity was developed by accounting for the effect of each of the girder pairs within the system. The system rigidity for a single pair of adjacent girders is shown in Eq. 12:

$$\frac{EI_x s^2}{2} \tag{12}$$

To evaluate the vertical warping rigidity of a girder system, girders are idealized to be "paired" with a counterpart that is an equal distance from the centroid of the system. Eq. 12 can be modified for any girder pair by using the appropriate distance between the two girders. It is assumed that the centroids of the girder pair and the system coincide. For a system with an even number of girders, the centroid is located midway between the girder pairs; while a system with an odd number of girders will have a centroid that is coincident with the center girder. The distance between a given girder pair (s_i) is found by multiplying the girder spacing (s) by the number of spaces between them. Figs. 3 and 4 show that the distance between any girder pair is the overall width of the system (sn_g-s) decreased by two girder spaces ($2s$) for each girder pair moved toward the center of the system.

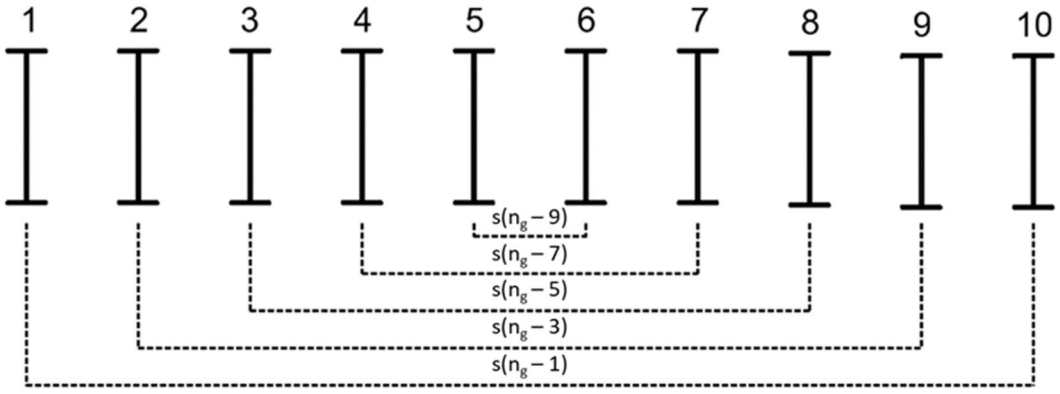

Figure 3: Example Girder Pairs for an Even Number of Girders (Fish, 2021)

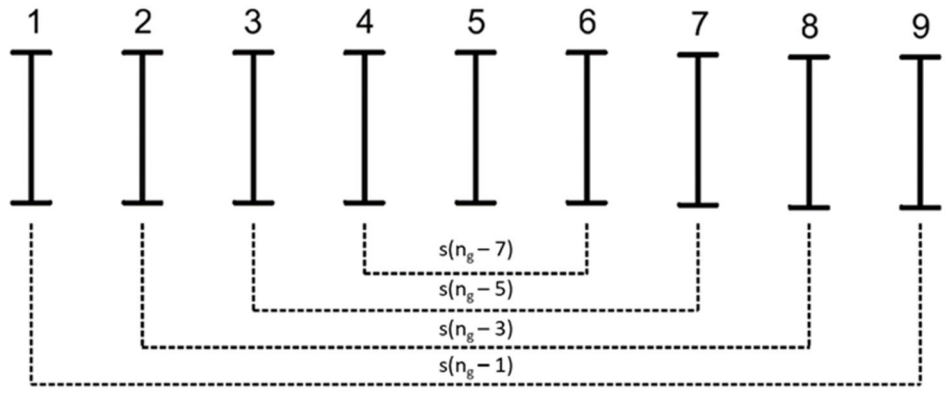

Figure 4: Example Girder Pairs for an Odd Number of Girders (Fish, 2021)

From this, a system warping stiffness factor was developed and is as follows:

$$\alpha_x = \sum \left(n_g - i\right)^2 \tag{13}$$

where the index (i) represents each odd number that is less than n_g.

The first five system warping stiffness factors are provided in Table 1.

Table 1: System Stiffness Warping Factors (α_x)

Number of Girders[1]	Associated Values of i	α_x
2	1	1
3	1	4
4	1,3	10
5	1,3	20
6	1,3,5	35

1. Eq. 13 can be used to determine factors for systems with more than 6 girders.

Multiplying the system warping stiffness factor (Eq. 13) by the system rigidity for a single pair of girders (Eq. 12) results in the vertical warping rigidity of a system of multiple girders.

Substituting all three of the modified system rigidities into Eq. 1, and dividing by the number of girders in the system, leads to the following expression for system buckling capacity on a per girder basis (Eq. 14):

$$M_{g,n_g} = \frac{\pi}{L_g}\sqrt{EI_yGJ + \left[\frac{\pi^2 E^2 I_y}{L_g^2}\right] * \left[\frac{I_y h_o^2}{4} + \frac{\alpha_x}{n_g}\frac{I_x s^2}{2}\right]} \tag{14}$$

Note that, for a single girder system, n_g = 1 and s = 0. In this case, Eq. 14 reduces to M_o and is equivalent to Eq. 1.

As described regarding the development of Eq. 4, the effect of the St. Venant term in Eq. 14 is generally small and can be considered negligible. Neglecting this term, Fish (2021) produced the simplified expression shown in Eq. 15 which gives the simplified buckling moment capacity for a girder in a system comprised of any number of girders:

$$M_{gs,n_g} = \frac{\pi^2 sE}{L_g^2}\sqrt{I_y I_x\left(\frac{\alpha_x}{2n_g}\right)} \tag{15}$$

3.2 Derivation of a Refined In-Plane Girder Stiffness Expression

There are two common ways of computing the buckling capacity of beams. The system buckling capacity derived in the previous section (Eq. 14) is similar to Timoshenko's solution (Eq. 1), which is the most common approach. The other common way is to utilize Eq. 11, which relates the buckling capacity of a beam(s) to the total system stiffness. Recalling Eq. 9, it can be seen that, by isolating the in-plane girder stiffness component, Eq. 11 can be used to develop an expression for the in-plane girder stiffness.

To develop an expression for the in-plane stiffness using a continuous bracing approach, an assumption was made that the brace and cross-sectional distortion stiffness components were significantly larger than the in-plane stiffness component, β_g. In such a case, the equation for springs in series tends to the following:

$$\frac{1}{\bar{\beta}_T} = \frac{1}{\bar{\beta}_g} \tag{16}$$

where $\bar{\beta}_g$ is the continuous in-plane girder stiffness (with units of moment/radian/unit-length) and $\bar{\beta}_T$ is as previously defined.

By substituting Eq. 16 into Eq. 11, the critical buckling capacity becomes a function of the continuous in-plane girder stiffness alone (Eq. 17):

$$M_{cr} = \sqrt{M_o^2 + \bar{\beta}_g EI_y} \tag{17}$$

By setting Eq. 14 and Eq. 17 equal to one another, an expression for the continuous in-plane girder stiffness can be derived explicitly (Eq. 18):

$$\bar{\beta}_g = \frac{\pi^4 EI_x s^2}{2n_g L_g^4}\alpha_x \tag{18}$$

$\bar{\beta}_g$ is, again, a continuous stiffness. In order to discretize this so that it can be attributed to a single brace location, an adjustment of L_g/n_{cf} was used. The resulting expression is:

$$\beta_{g,new} = \frac{\pi^4 E I_x s^2}{2 n_g n_{cf} L_g^3} \alpha_x \tag{19}$$

4. Verification Studies

Two finite element studies were utilized in the investigation to evaluate the accuracy of the solutions. The program mBrace3D (2021) was used in the first study while Abaqus (2022) was used in the second. The results of the first study are provided in Fish (2021). This paper primarily focuses on the results from the second study that targeted the system stiffness behavior. In both the mBrace3D and Abaqus models, the girders were interconnected with torsional bracing in the form of cross-frames. The models therefore represent the common critical loading stage during deck placement when the steel sections alone resist the full construction loading.

4.1 In-Plane Girder Stiffness from a System Buckling Perspective

The following subsections briefly describe the verification study performed by Fish (2021). This study, which is described in detail in Fish (2021), used the program mBrace3D to verify the newly developed continuous in-plane girder stiffness expression's (Eq. 18) ability to predict the system buckling capacity of a range of girder systems.

4.1.1 Finite Element Model

The finite element program mBrace3D (2021) was used to study the buckling behavior of multi-girder systems that utilize torsional braces (cross-frames in this case) for stability and linear-elastic materials were used in all cases.

The same boundary conditions were used for all models and are illustrated in Fig. 5. All girders were simply supported in-plane and all cross-frames were connected perpendicular to the girders. At the supports, all girders were pinned in the out-of-plane direction at the top and bottom web-to-flange intersection. This restraint prevents girder twist while allowing for warping, which matches the assumptions made when deriving both Eqs. 1 and 14.

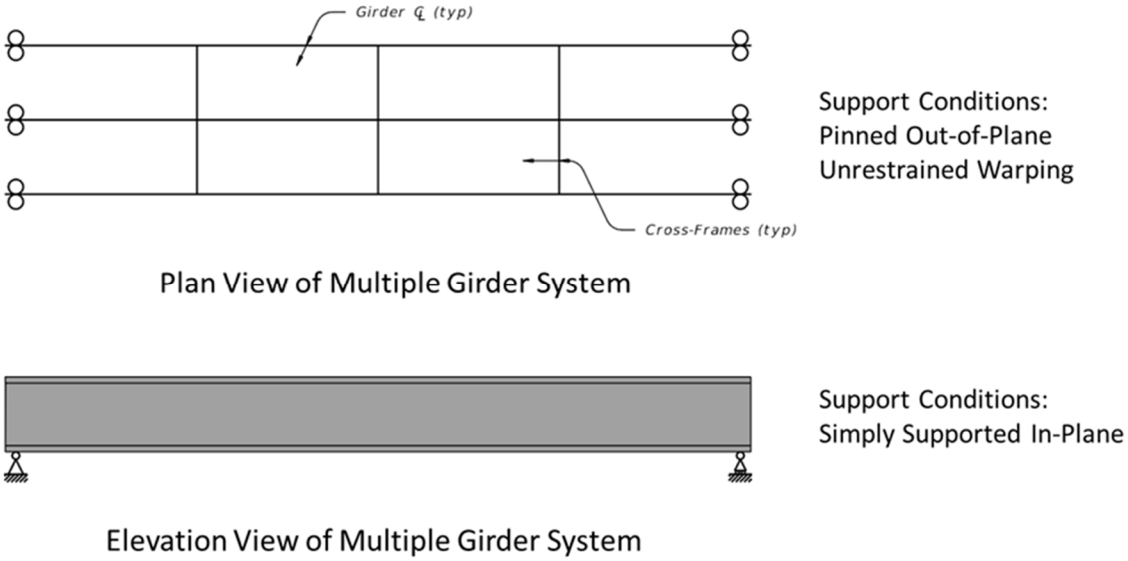

Figure 5: Assumed Finite Element Model Boundary Conditions (Fish, 2021)

The four cross-sections considered are shown in Fig. 6, which consist of doubly-symmetric I-shaped sections. There have been recent studies on the effects of girder mono-symmetry on the LTB behavior (Reichenbach et al., 2020) and it is expected that the results of those studies are similarly applicable here.

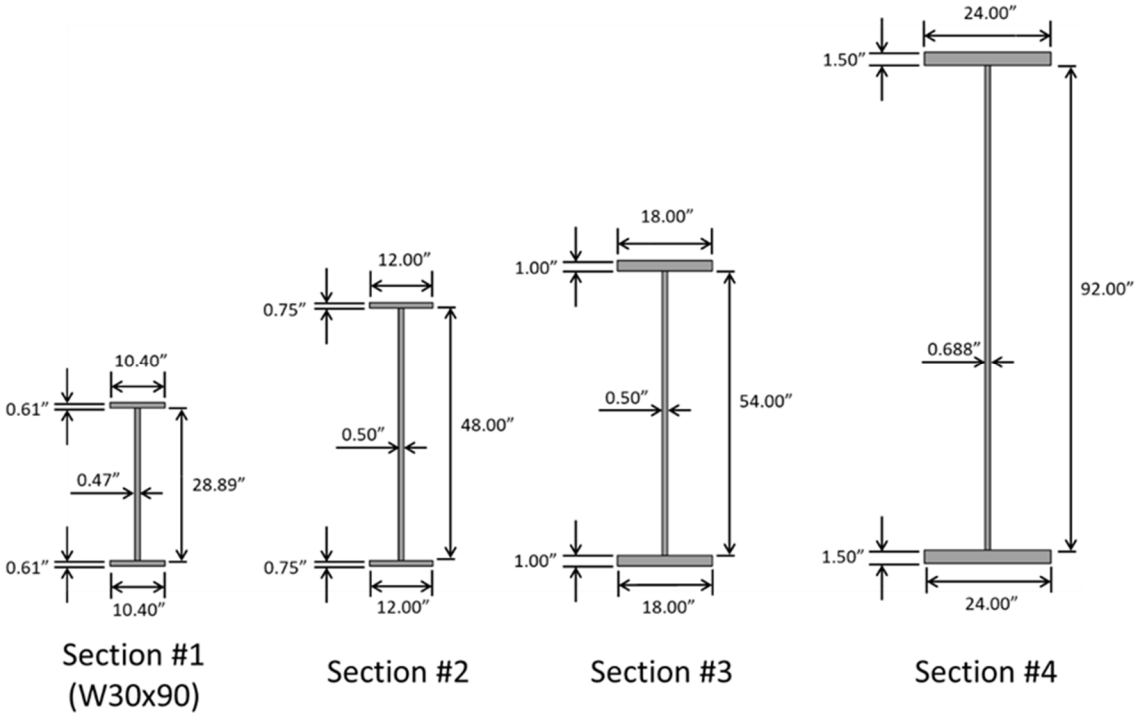

Figure 6: I-Girder Cross-Sections Analyzed in Initial Study (Fish, 2021)

4.1.2 Effect of Number of Cross-Frames

As stated previously, a few assumptions were made in the development of Eq. 14. Chief among them is that there are enough cross-frames supplied along the length of the girder such that system distortion between the brace locations can be assumed to be negligible.

Fig. 7 shows the comparison of finite element analysis results as compared to the predicted results of Eq. 14 for the given system. The vertical axis represents the critical system buckling moment on a per-girder basis (M_{cr}), normalized by the critical buckling moment of a single, unbraced girder (M_o) and the horizontal axis represents the number of girders the system has across its width.

Fig. 7 also shows that, when the cross-frame spacing is small, the new in-plane girder stiffness expression almost exactly predicts the system buckling capacity. However, when there are very few cross-frames (or when cross-frame spacing is large), the derived expression tends to overestimate the buckling capacity. This overestimation can become significant for wide systems with very few cross-frame lines.

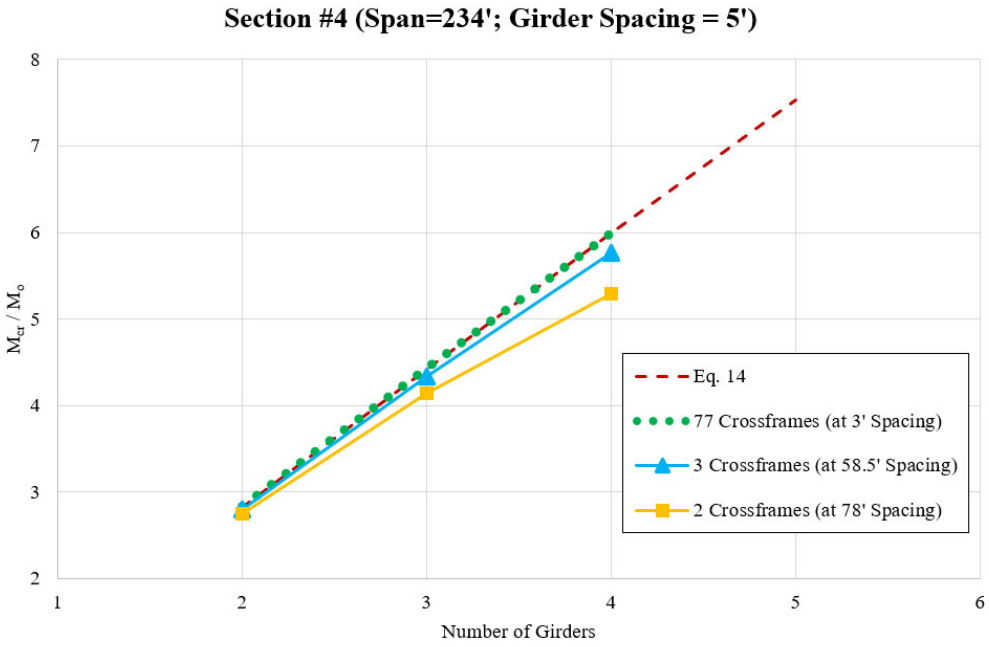

Figure 7: Normalized Buckling Capacity as a Function of Number of Girders and Cross-Frames

4.1.3 Effect of Brace Stiffness

Another assumption that was made during the derivation of the new equations is that the brace stiffness is large enough that its impact on the overall system stiffness is negligible. Though there are, indeed, many cross-frame details that provide stiffness values that would satisfy this assumption, the general assumption is not universally true. So, it was also important to assess the impact of a range of brace stiffness values on the accuracy of these new equations.

To do this, a comparison of the current and new in-plane girder stiffness expressions was made by substituting each of them into Eq. 11. The two resulting expressions are below. Eq. 20 corresponds to the per-girder buckling moment predicted when using the current in-plane girder stiffness expression (Eq. 10) while Eq. 21 corresponds to the new expression (Eq. 19).

$$M_{cr,current} = \sqrt{M_o^2 + \frac{EI_{eff}\, n_{cf}}{L_g\left(\frac{1}{\beta_{b,act}} + \frac{1}{\beta_{sec}} + \frac{1}{\beta_{g,current}}\right)}} \tag{20}$$

$$M_{cr,new} = \sqrt{M_o^2 + \frac{EI_{eff}\, n_{cf}}{L_g\left(\frac{1}{\beta_{b,act}} + \frac{1}{\beta_{sec}} + \frac{1}{\beta_{g,new}}\right)}} \tag{21}$$

Examples of the predicted behavior using Eqs. 20 and 21 are shown in Fig. 8.

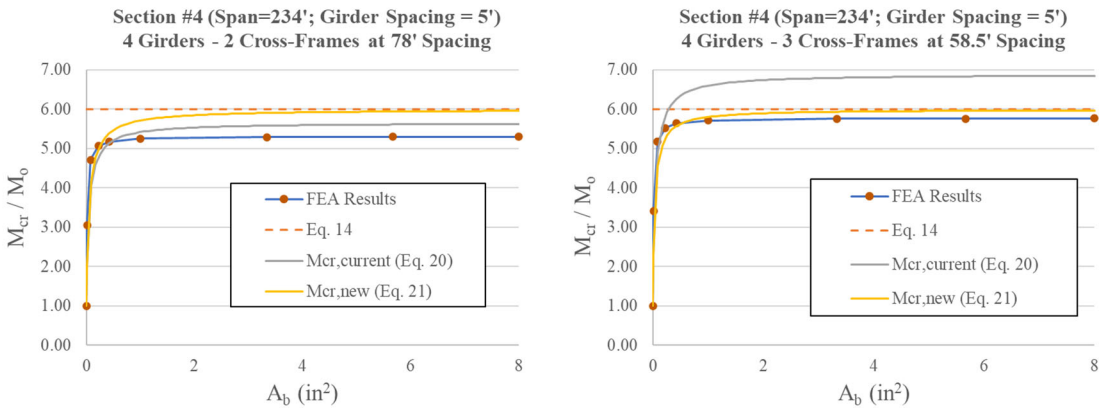

Figure 8: Current In-Plane Girder Stiffness Expression Compared to the New Version

An overall trend is that the current expression (Eq. 20) has good agreement for the case with only two cross-frames but becomes more unconservative as more cross-frames are added. This trend is plausible since the current in-plane girder stiffness expression was derived for a twin-girder system with a single cross-frame at mid-span. Another trend is that the new expression (Eq. 21) works well as more cross-frames are added. Although only cases with two and three intermediate cross-frame lines are shown in Fig. 8, these trends became more significant with increasing numbers of cross-frame lines.

4.1.4 Adjustment to the New In-Plane Girder Stiffness Expression

The results in the last section demonstrated that the current expression provides reasonable predictions of the global buckling moment of systems with relatively few cross-frames but becomes unconservative with increasing number of cross-frame lines. On the contrary, the new solution is unconservative for cases with few cross-frame lines and becomes more accurate with increasing bracing lines. Therefore, a linear transition adjustment (C_n) was developed such that a proposed expression would agree with the current one (Eq. 10) for cases of one intermediate cross-frame and agree with the new expression (Eq. 19) when there are many intermediate cross-frames. In this adjustment expression, it is assumed that the full transition from Eq. 10 to Eq. 19 is achieved when the system has more than four intermediate cross-frames.

$$C_n = \frac{(n_g - 1)^2}{2\alpha_x}\left(1 + \frac{1 - n_{cf}}{4}\right) + \frac{n_{cf} - 1}{4} \tag{22}$$

Applying this modification to Eq. 19 results in the following expression:

$$\beta_{g,prop} = \frac{\pi^4 E I_x s^2}{2 n_g n_{cf} L_g^3} C_n \alpha_x \tag{23}$$

The next subsection documents the verification process of this proposed expression (Eq. 23).

4.2. Finite Element Study on In-Plane Girder Stiffness

As discussed earlier, the current in-plane girder stiffness expression (Eq. 10) was derived for a twin-girder system with a single brace at midspan. Therefore, the accuracy of the current equation for multiple girder systems with multiple intermediate braces needs to be verified. In this section, parametric studies were carried out in Abaqus (2022) to investigate the in-plane girder stiffness of various I-girder systems.

4.2.1 Finite Element Model

The variables considered in the study included number of girders, number of intermediate cross-frames (n_{cf}), girder spacing, and flange width-to-web depth ratio (b/d). Table 2 presents the range of each parameter, which are representative of values used in practice.

Table 2: Parameters considered in the parametric study

Parameter	Range of Values
Span length [ft]	160
Number of girders	2, 3, 4, 5
Number of n_{cf}	1, 2, 3, 4, 5
Girder spacing	8, 10, 12, 40
Span-to-depth ratio	25
Flange width-to-web depth ratio	1/6, 1/4

In the FE models, the cross-sections of the girders (i.e., web, flanges, and stiffeners) were modeled with shell elements, and cross-frames were modeled with truss elements. A representative section is shown in Fig. 9. The girders were simply supported with twist restrained by preventing lateral movement at the top and bottom of the webs. The analysis consisted of eigenvalue buckling analyses to study the stiffness behavior of the cross-frame system. The girders were subjected to uniform moment loading by providing a force couple at the ends of the beams. A major aspect of the FEA studies was developing a methodology of separating the effects of cross-sectional distortion, brace stiffness, and in-plane girder stiffness and to determine the ideal brace stiffness for the bracing system. The effects of cross-sectional distortion were eliminated by using full depth cross frames. However, the system still is impacted by both the brace stiffness and the in-plane stiffness. The following subsection outlines the procedure of isolating the stiffness of the brace from the in-plane stiffness of the girder.

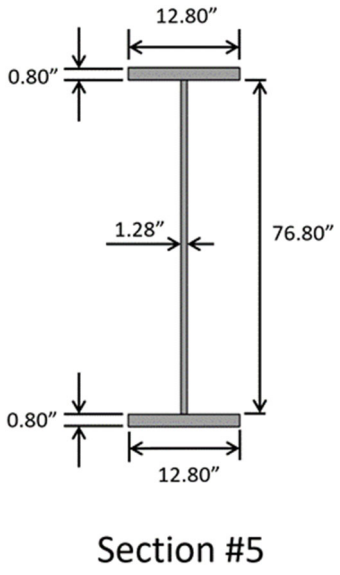

Figure 9: An I-Girder Cross-Section Analyzed in Verification Study

4.2.2 In-Plane Girder Stiffness

This section discusses the method by which the in-plane girder stiffness component was isolated from the entire bracing system stiffness using FE models. As noted previously in Equation (9), the total brace stiffness is a combination of β_b, β_{sec}, and β_g. As noted in the last section, full depth cross-frames were utilized so that web distortion did not impact the behavior. In the balloted AASHTO bracing provisions, cross-sectional distortion can be ignored provided the braces are deeper than 80% of the web depth, which is consistent with the modelling used in this study. Because the in-plane girder stiffness increases with wider girder spacing, selecting a large girder spacing can result in the in-plane stiffness to be suitably large to be considered "infinite". To achieve this, a girder spacing of 40 ft. was selected, which allowed the total brace stiffness to be considered equal to the cross-frame stiffness (β_b) alone, since β_{sec} and β_g are assumed to be infinity. For the other spacing systems (i.e., 8, 10, and 12 ft spacing systems), β_g can be obtained by the following expression:

$$\frac{1}{\beta_T} = \frac{1}{\beta_{b,ideal}} + \frac{1}{\beta_g} \tag{24}$$

where β_T is the ideal cross-frame stiffness from 40ft spacing system from FEA, $\beta_{b,ideal}$ is the ideal cross-frame stiffness from FEA, and β_g is the calculated in-plane girder stiffness.

Table 3 shows an example of the calculations of in-plane girder stiffness based on the FEA results.

Table 3: Example of in-plane girder stiffness calculation [k-in/rad]

System	$\beta_{b,ideal}$ from FEA	β_T (= $\beta_{b,40ft}$)	β_g
8ft	25,107	14,978	37,125
10ft	20,091		58,852
12ft	18,055		87,874
40ft	14,978		∞

4.2.3 Parametric Study Results

In-plane girder stiffness results from three different girder systems are presented in this section (Figs. 10 through 12). The plots below compare the in-plane girder stiffness from: FEA solutions, the current expression (Eq. 10), the unmodified expression (Eq. 19), and the proposed expression (Eq. 23). Each of the subject systems was analyzed at girder spacings of 8, 10, and 12ft. The graphs show the impact of the adjustment factor, C_n. For the case in Fig. 10 with a single cross-frame at midspan, the current expression (Eq. 10) and the proposed expression are coincident. The other two graphs in Figs. 11 and 12 show respective results for the cases with 3 and 5 cross-frames. In the case with 5 cross-frames, the proposed solution is coincident with Eq. 19.

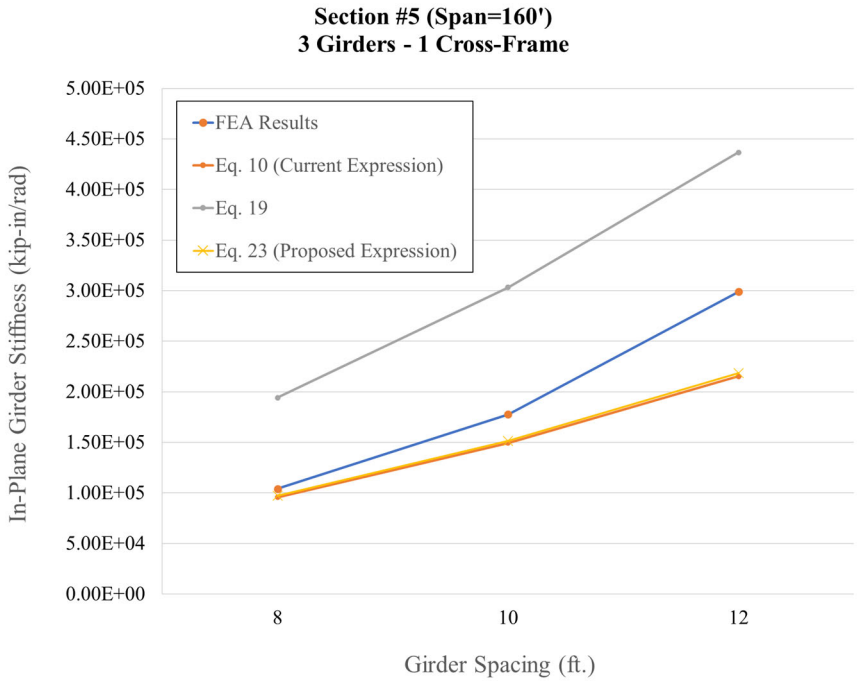

Figure 10: In-Plane Girder Stiffness Predictions for a 3-Girder System with 1 Intermediate Cross-Frame

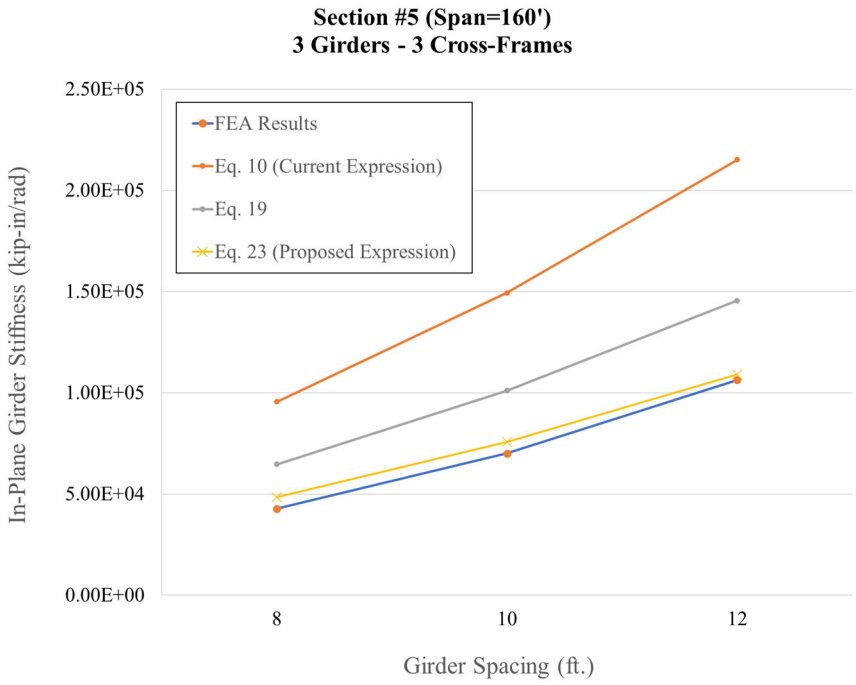

Figure 11: In-Plane Girder Stiffness Predictions for a 3-Girder System with 3 Intermediate Cross-Frames

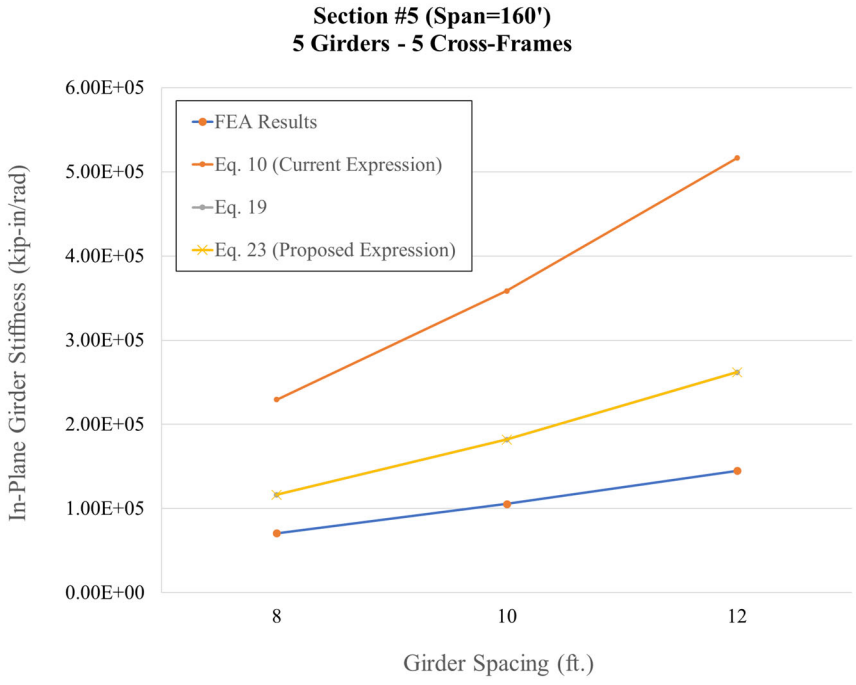

Figure 12: In-Plane Girder Stiffness Predictions for a 5-Girder System with 5 Intermediate Cross-Frames

In the three previous figures, the FEA results are considered to be an accurate representation of the true in-plane girder stiffness attributed to each girder within the system. Any predicted results by the derived solutions that are greater in magnitude than those of the FEA results are overpredicting the available in-plane girder stiffness and are, therefore, unconservative. The

opposite is also true; any results predicted by the derived expressions are considered to be conservative if they are less than those of the FEA results.

As noted above, when the system being analyzed has only one intermediate cross-frame, the current and proposed in-plane girder stiffness expressions are nearly identical to one another, and the predictions will typically be somewhat conservative. In general, when there are multiple cross-frames present, the current expression tends to be unconservative and gets more so as cross-frames are added.

For narrow girder systems, the proposed expression (Eq. 23) tends to become more accurate as cross-frames are added. However, as the system becomes less narrow, the proposed expression becomes somewhat unconservative. Though this is currently the case, the proposed expression is much less unconservative than the current expression. Work is ongoing to better refine this expression.

5. Conclusions

In this paper, a new in-plane girder stiffness expression was derived, and its accuracy was investigated. This proposed expression was also compared to the current in-plane girder stiffness expression, which is being considered for inclusion in the upcoming AASHTO edition. The current expression was found to be accurate for situations in which there was one intermediate cross-frame in the system. This was in-line with expectations since the current expression was derived for a twin-girder system with a single cross-frame at mid-span. However, the current expression proved to be unconservative in many cases with multiple intermediate cross-frames.

The proposed expression has thus far shown good agreement with finite element analysis solutions, particularly when the system is narrow. There have been cases identified where the proposed expression is unconservative, however it is consistently much less unconservative than the proposed expression. Though work is ongoing, the proposed expression has shown better agreement with finite element analysis results than its current counterpart and is, therefore considered to offer a more accurate solution.

Acknowledgements

The authors would like to thank the Texas Department of Transportation for funding the lead author to conduct the work on this paper as part of the educational program. Any opinions, findings, and conclusions or recommendations expressed in this material are those of the authors and do not necessarily reflect the views of the Texas Department of Transportation.

References

AASHTO (2020) *LRFD Bridge Design Specifications*. 9th edn. Washington, DC: American Association of State Highway and Transportation Officials.

Abaqus Unified FEA (2022). Available at: https://www.3ds.com/products-services/simulia/products/abaqus/.

AISC (2016) *Specification for Structural Steel Buildings*. Chicago: American Institute of Steel Construction.

AISC (2022) *Code of Standard Practice*. Chicago: American Institute of Steel Construction.

Biju-Duval, P. (2017) *Development of Three-Dimensional Finite Element Software for Curved Plate Girder and Tub Girder Bridges During Construction*. Dissertation. University of Texas at Austin.

Biju-Duval, P. (2021) mBrace3D. Available at: https://www.mbrace3d.com/.

Fish, D.J. (2021) *Refined Design Expressions for In-Plane Girder Stiffness and System Buckling Capacity*. Master's Thesis. University of Texas at Austin.

Han, L. and Helwig, T. (2016) *Effect of Girder Continuity and Imperfections on System Buckling of Narrow I-girder Systems*. Annual Stability Conference Structural Stability Research Council, Orlando, FL, p. (10 pages).

Helwig, T., Yura, J. and Frank, K. (1993) *Bracing Forces in Diaphragms and Cross Frames*, Structural Stability Research Council Conference "Is Your Structure Suitably Braced?", pp. 129–140.

Helwig, T.A. and Wang, L. (2003) *Cross-Frame and Diaphragm Behavior for Steel Bridges with Skewed Supports*. Research Report 1772–1. Report for Texas Department of Transportation.

Reichenbach, M. et al. (2020) *Lateral-Torsional Buckling of Singly Symmetric I-Girders with Stepped Flanges.* ASCE Journal of Structural Engineering, 146(10), pp. 04020203-1-15 (15 pages).

Taylor, A.C. and Ojalvo, M. (1966) *Torsional Restraint of Lateral Buckling.* Journal of the Structural Division, ASCE, ST2, pp. 115–129.

Timoshenko, S. and Gere, J. (1961) *Theory of Elastic Stability*. New York: McGraw-Hill.

Wang, L. and Helwig, T.A. (2005) *Critical Imperfections for Beam Bracing Systems.* Journal of Structural Engineering, 131(6), pp. 933–940.

Winter, G. (1960) *Lateral Bracing of Columns and Beams.* ASCE Transactions, 125, pp. 809–825.

Yura, J.A. (2001) *Fundamentals of Beam Bracing*. Eng. J.; 11-26

Yura, J.A. et al. (2008) *Global Lateral Buckling of I-Shaped Girder Systems.* Journal of Structural Engineering, 134(9), pp. 1487–1494.

Yura, J.A. (1992) *Bracing of Steel Beams in Bridges*. 1239–4F. Texas Department of Transportation, p. 96.